General Solutions to the Navier-Stokes Equations for Incompressible Flow

JangRyong Shin[1]

[1]*Engineer, Offshore structure design department, Hanwha Ocean Co., LTD, Geoje, Korea*

ABSTRACT: *Waves are mainly generated by wind via the transfer of wind energy to the water through friction. When the wind subsides, the waves transition into swells and eventually dissipate. Friction plays a crucial role in the generation and dissipation of waves. Numerous wave theories have been developed based on the assumption of inviscid flow, but these theories are inadequate in explaining the transformation of waves into swells. This study addressed these limitations by analytically deriving general solutions to the Navier–Stokes equations. By expressing the velocity field as the product of a solution to the Helmholtz equation and a time-dependent univariate function, the Navier–Stokes equations are decomposed into an ordinary differential equation and the Euler equations, which are solved using tensor calculus. This paper provides solutions for viscous flow with shear currents when applied to the water wave problem. These solutions were validated through their application to the vorticity equation. The decay modulus of water waves was compared with experimental data, showing a significant degree of concordance. In contrast to other wave theories, this study clarified the process through which waves evolve into swells.*

1. Introduction

Water waves are considered one of the most fascinating natural phenomena in the marine environment. Waves in the open ocean are generally generated by winds. The transmission of energy from the wind to the water is facilitated by friction between these two fluid media. This energy is transmitted as a wave across the water surface. Consequently, friction plays a pivotal role in the circulation of fluids and is a crucial factor in wave generation. The energy transferred from the wind to waves diminishes as the wind intensity decreases, leading to the transformation of waves into swells that eventually dissipate. Therefore, friction also contributes to the dissipation of waves. Nevertheless, the mathematical description of water waves has been conducted under the assumption of irrotational, inviscid flow (Chaplin, 1980; Chappeleakimr, 1961; De, 1955; Dean, 1965; Fenton, 1988; Kishida and Sobey, 1988; Korteweg and de Vries, 1895; Rienecker and Fenton, 1981; Shin, 2016, 2019; Stokes, 1847; Stoke, 1880; Skjelbreia and Hendrickson, 1960; Vanden-Broeck and Schwartz., 1979) or under the assumption of rotational, inviscid flow (Rankine, 1863; Chen and Zou, 2019; Constantin, 2005; Dalrymple, 1974; Henry; 2008; Nwogu, 2009; Shin, 2022, 2023). Hence, these studies cannot account for the natural dissipation of waves. In a few exceptional cases, viscosity is considered in the linearized Navier-Stokes equations, e.g., water waves over a viscous mud bottom and seiche phenomena in coastal regions. The equation (Dean and Dalrymple, 1984) for long waves with bottom friction is analogous to that of a damped harmonic oscillator. The amplitude decreases exponentially with time, and the angular frequency also changes, providing an important clue for solving the Navier−Stokes (NS) equations. NS equations are a set of nonlinear partial differential equations that govern the flow of Newtonian fluids. These equations are valuable because of their ability to elucidate numerous physical phenomena. The structural design process commences by evaluating the external appearance of the design object and the loads on the surface generated by fluid flow. The NS equations are used for these determinations. Despite the wide range of practical applications, the existence of smooth solutions in three dimensions has not been proven definitively. Theoretical solutions remain limited for most cases, with only a few exceptions. Analytical approaches are deemed almost impossible for solving these problems. Thus, only numerical and experimental methods are allowed. This study applied a theoretical approach with tensor calculus to address these limitations. General solutions were introduced without considering the boundary conditions and initial conditions.

NS equations are the Euler equations with the addition of the gradient of the viscous stress tensor. The viscous stress tensor is proportional to the strain rate, making the gradient of viscous stress a

linear function of the velocity field. The convective acceleration is the only nonlinear term included in the Euler equation. Shin (2022, 2023) reported the complete solutions to the Euler equations. They transformed the Euler equations into Bernoulli's principle when the velocity field was described by the solutions of the Helmholtz equation. Using the methodology used in the studies conducted by Shin (2022, 2023) with the solution for a damped harmonic oscillator, the findings were extended to cover general three-dimensional viscous flow in the current study.

When the velocity field is described by solutions of the Helmholtz equation, the gradient of the viscous stress tensor for incompressible flow is proportional to the velocity field. The product of a solution to the Helmholtz equation and any time function is also a solution to the Helmholtz equation. By substituting the product into the NS equations, these equations can be decomposed into the Euler equations and a linear ordinary differential equation for the time function. Based on Shin's (2022) research, this study solved the Euler equations for general flow. Some exact solutions to NS equations exist. The Taylor–Green vortex (Taylor and Green, 1937) and Antonio's solution (Antuono, 2020) are two interesting examples. The Taylor–Green vortex was an unsteady flow of a decaying vortex in Cartesian coordinates. Antonio's solution is considered a three-dimensional generalization of the classic two-dimensional Taylor–Green vortex. For verification, the Taylor–Green vortex and Antonio's solutions are special cases of the solutions presented in this study. Substituting the results into the vorticity equations confirmed that the vorticity equations were satisfied.

This study adjusted Shin's results (2022, 2023) to comply with NS equations. The process through which waves evolve into swells was elucidated. The modified wave theory was verified by comparing the decay modulus with the experimental data of Shiau and Rumer (1974) and the theoretical solution presented by Dean and Dalrymple (1984). The comparison results showed a high level of agreement.

2. Navier-Stokes Equations for Incompressible Flow

Tensor notation was used for simplicity, and the following rule was adopted when using tensor notation. Whenever the subscript appeared twice as a letter in a grouping, the expressions of this grouping were summed, with the repeated index taking on successively the values 1, 2, and 3. The non-repeated letter subscripts or numerical subscripts remain fixed during the process (Dym and Shames, 1973). The partial derivatives of a tensor are denoted using commas and indices as $\frac{\partial(\ )}{\partial x_i} = (\ )_{,i}$ where x_i is the position vector; the conservation of mass is presented as follows:

$$v_{i,i} = 0 \tag{1}$$

where v_i is the velocity field, which is a vector function of position, x_i,

and time, t. The conservation of momentum is presented as follows:

$$\dot{v}_i + v_j v_{i,j} = -\frac{p_{,i}}{\rho} + \mu v_{i,jj} + f_i \tag{2}$$

A time derivative will be denoted with the 'over-dot' notation. Therefore, $\dot{v}_i$ is the local acceleration. ρ is the density of the fluid, which is a constant; $p = p(x_i, t)$ is pressure field; μ is kinematic viscosity, which is a constant; f_i is body force per unit mass, which is a conservative force. The NS equations for an incompressible fluid are composed of Eqs. (1) and (2). The vorticity is defined as follows:

$$\Omega_i \overset{\text{def}}{=} \epsilon_{ipq} v_{q,p} \tag{3}$$

where ϵ_{ipq} is the Levi−Civita symbol. Taking the inner product of the vorticity and the Levi-Civita symbol results in

$$v_{q,p} = v_{p,q} + \Omega_i \epsilon_{ipq} \tag{4}$$

Taking the inner product of the velocity v_p and the deformation tensor $v_{q,p}$, the convective acceleration in Eq. (2) is expressed as

$$v_p v_{q,p} = v_p v_{p,q} + v_p \Omega_i \epsilon_{ipq} \tag{5}$$

Replacing $p = j$, $q = i$, and $i = k$, Eq. (5) can be presented as follows because $v_p \Omega_i \epsilon_{ipq} = v_p \Omega_i \epsilon_{qip} = -v_p \Omega_i \epsilon_{qpi}$:

$$v_j v_{i,j} = v_j v_{j,i} - \epsilon_{ijk} v_j \Omega_k \tag{6}$$

Substituting Eq. (6) into Eq. (2), the alternative form of the momentum equation is represented as follows:

$$\dot{v}_i + v_j v_{j,i} + \frac{p_{,i}}{\rho} - f_i = \epsilon_{ijk} v_j \Omega_k + \mu v_{i,jj} \tag{7}$$

Because f_i is a conservative force, it has potential energy. The first term on the right-hand side represents the outer product of the velocity and vorticity. Therefore, the term is zero when the vorticity and the velocity are parallel to each other.

3. Decomposition of the Navier-Stokes Equations

A definitive clue to solving the NS equations can be found in the solution of a single-degree-of-freedom damped harmonic oscillator or long waves with bottom friction (Dean and Dalrymple, 1984). In the oscillator, the damping force is proportional to the velocity $\dot{z}$ of the object because it is due to fluid viscosity: $-c\dot{z}$, where c is the damping coefficient. Newton's second law for a damped harmonic oscillator is presented as follows:

$$\ddot{z} + 2\xi\omega\dot{z} + \omega^2 z = 0 \tag{8}$$

where ω is the undamped angular frequency of the oscillator, and ζ is the damping ratio. The displacement is expressed as

$$z(t) = Ae^{-\xi\omega t}\sin\left(\sqrt{1-\xi^2}\,\omega t + \phi\right) \tag{9}$$

where A is the amplitude, ϕ is the phase, and $e^{-\xi\omega t}$ is the exponential decay of the amplitude. Eq. (9) indicates that the damping force reduces the natural frequency, decreases the amplitude, and eventually eliminates the oscillation. Considering that the gradient of viscous stress in Eq. (7) arises from a Newtonian fluid, similar to the oscillator, the solutions to the NS equations are presented in a similar form to Eq. (9). If the velocity field is a solution to the Helmholtz equation, i.e., $v_{i,jj} = bv_i$, the gradient of viscous stress is presented as $\mu v_{i,jj} = \mu bv_i$, where b is a constant with the unit of inverse area. Therefore, like the damped harmonic oscillator, the gradient of viscous stress is proportional to the velocity field. Eq. (9) is based on the assumption that the velocity field for viscous flow is represented as follows:

$$v_i(t,x_1,x_2,x_3) \overset{\text{def}}{=} F(t)u_i(t,\ x_1,x_2,x_3) \tag{10}$$

where $F(t)$ is a function of time, which is a dimensionless quantity, and u_i is a velocity field for inviscid flow to satisfy the Helmholtz equation. Examples of u_i include the water particle velocities presented by Shin (2022, 2023).

Theorem 1. When the velocity fields are represented as a product of a time function and solutions of the Helmholtz equation, the NS equations can be decomposed into the Euler equations and an ordinary equation for the time function.

Proof. Substituting Eq. (10) into Eq. (1), the conservation of mass is presented as follows:

$$u_{i,i} = 0 \tag{11}$$

The gradient of viscous stress is presented as $\mu v_{i,jj} = \mu bv_i = \mu bF(t)u_i$, and the local acceleration is presented as follows:

$$\dot{v}_i = \dot{F}u_i + F\dot{u}_i \tag{12}$$

Substituting Eq. (12) and $\mu v_{i,jj} = \mu bF(t)u_i$ into Eq. (7), Eq. (7) is converted to the Euler momentum equation, provided that the following condition is satisfied:

$$\dot{F}u_i = \mu bFu_i \tag{13}$$

Because $u_i \neq 0$, the solution to Eq. (13) can be presented as follows:

$$F(t) = e^{\mu bt} \tag{14}$$

The constant, b, must be negative because the flow must eventually dissipate. Eq. (14) shows similarities to the exponential decay of the amplitude, as expressed in Eq. (9). Eq. (7) is presented as follows:

$$F\dot{u}_i + F^2 u_j u_{j,i} + \frac{p_{,i}}{\rho} - f_i = F^2 \epsilon_{ijk}u_j\overline{\Omega}_k \tag{15}$$

where the vorticity, $\Omega_k \overset{\text{def}}{=} F(t)\overline{\Omega}_k$. Therefore, $\overline{\Omega}_k = \epsilon_{kpq}u_{q,p}$.

Theorem 2. When the velocity field is a solution of the Helmholtz equation, then the vorticity is also a solution of the Helmholtz equation.

Proof. $\Omega_{i,jj} = (\epsilon_{ipq}v_{q,p})_{,jj} = (\epsilon_{ipq}v_{q,jj})_{,p} = (\epsilon_{ipq}bv_q)_{,p} = b(\epsilon_{ipq}v_{q,p}) = b\Omega_i$

As a result, the velocity field and the vorticity field were determined using the Helmholtz equation. The next step was to determine the pressure field using Eq. (15). "$0 < F(t) < 1$", and it has no dimensions. Hence, it is considered a non-dimensional perturbation parameter. Using the perturbation method, Eq. (15) can be solved in the following chapters for two cases: u_i is steady flow and u_i is unsteady flow.

4. Pressure Field for Steady Flow

When the velocity field, u_i is independent of time, Eq. (10) is presented as follows:

$$v_i(t,x_1,x_2,x_3) = F(t)u_i(x_1,x_2,x_3) \tag{16}$$

Therefore, the local acceleration in Eq. (15) is zero. The pressure field is presented as the sum of the dynamic pressure and static pressure. The pressure field must be presented by a quadratic function with respect to $F(t)$ because the dynamic pressure is proportional to the square of the velocity, and static pressure is proportional to the body force, as follows.

$$p \overset{\text{def}}{=} \rho S(x_1,x_2,x_3) + F^2(t)\rho D(x_1,x_2,x_3) \tag{17}$$

The first and second terms mean the static and dynamic pressures, respectively. Substituting Eqs. (16)–(17) into Eq. (15), the result is presented as

$$\{S_{,i} - f_i\} + \{D_{,i} + u_j u_{j,i} - \epsilon_{ijk}u_j\overline{\Omega}_k\}F^2 = 0 \tag{18}$$

Eq. (18) is decomposed with two equations because Eq. (18) is valid for all t, and $F(t) \neq 0$, using the perturbation method, as follows. The zero-order perturbation equation is presented as follows:

$$S_{,i} = f_i \tag{19}$$

The second-order perturbation equation is presented as

$$D_{,i} + u_j u_{j,i} - \epsilon_{ijk}u_j\overline{\Omega}_k = 0 \tag{20}$$

Integrating Eq. (19), the potential energy of the body force is determined as follows:

$$S = f_i x_i \tag{21}$$

The static pressure field is determined using Eq. (21). u_i is a solution of the Helmholtz equation. Hence, $u_{j,pp} = b u_j$. Therefore, the last term of Eq. (20) is presented as follows:

$$\epsilon_{ijk} u_j \overline{\Omega}_k = \frac{1}{b} \epsilon_{ijk} u_{j,pp} \overline{\Omega}_k \tag{22}$$

Using Eq. (4),

$$u_{j,pp} = \left(u_{p,j} + \overline{\Omega}_r \epsilon_{rpj} \right)_{,p} = u_{p,pj} + \overline{\Omega}_{r,p} \epsilon_{rpj} \tag{23}$$

Using Eq. (11), $u_{p,pj} = 0$, and $u_{j,pp} = \overline{\Omega}_{r,p} \epsilon_{rpj}$. Substituting it into Eq. (22),

$$\epsilon_{ijk} u_j \overline{\Omega}_k = \frac{1}{b} \epsilon_{ijk} \epsilon_{rpj} \overline{\Omega}_{r,p} \overline{\Omega}_k = \frac{1}{b} \left(\delta_{kr} \delta_{ip} - \delta_{kp} \delta_{ri} \right) \overline{\Omega}_{r,p} \overline{\Omega}_k \tag{24}$$
$$= \frac{1}{b} \left(\overline{\Omega}_k \overline{\Omega}_{k,i} - \overline{\Omega}_k \overline{\Omega}_{i,k} \right)$$

Where δ_{ij} is the Kronecker delta. Since divergence of curl is zero, we have $\overline{\Omega}_{k,k} = 0$. Therefore, $\overline{\Omega}_k \overline{\Omega}_{i,k} = (\overline{\Omega}_k \overline{\Omega}_i)_{,k}$. Let's introduce a quantity, $E_{,i} \overset{\text{def}}{=} (\overline{\Omega}_k \overline{\Omega}_i)_{,k}$. Therefore, $E = \int (\overline{\Omega}_k \overline{\Omega}_i)_{,k} \, dx_i$ is a type of kinetic energy. Because $\overline{\Omega}_k$ is also a solution of the Helmholtz equation and is determined by the velocity field, the energy, E can be easily determined. Substituting Eq. (24) into Eq. (20), the result is presented as follows.

$$D_{,i} + u_j u_{j,i} - \frac{1}{b} \left(\overline{\Omega}_k \overline{\Omega}_{k,i} - E_{,i} \right) = 0 \tag{25}$$

Bernoulli's principle can be expressed as Eq. (26) by integrating Eq. (25) with respect to x_i:

$$D + \frac{1}{2} u_j u_j - \frac{r}{2b} \overline{\Omega}_k \overline{\Omega}_k = Q(t) \tag{26}$$

The dynamic pressure field is determined using Eq. (26). The second term represents the kinetic energy associated with irrotational motion. In contrast, the third term represents the kinetic energy related to the vortex. The total kinetic energy is the linear sum of the two terms because the constant, b is negative, which is consistent with the law of conservation of energy. The ratio, r, is defined as

$$r \overset{\text{def}}{=} 1 - \frac{2E}{\overline{\Omega}_k \overline{\Omega}_k} \tag{27}$$

$\overline{\Omega}_k \overline{\Omega}_k \geq 2E \geq 0$ because the kinetic energy is a positive-definite function and the constant, b, is negative. Therefore $0 \leq r \leq 1$.

The energy E is referred to as an anti-vortex energy because it reduces the kinetic energy due to the vortex like frictional energy. Two cases of anti-vortex energy are considered as follows:

4.1 Anti-Vortex Energy Zero Case
$\overline{\Omega}_1 = \overline{\Omega}_2 = 0$ and $\overline{\Omega}_{3,3} = 0$ for 2-dimensional flow. Hence,

$$\overline{\Omega}_k \overline{\Omega}_{i,k} = 0 \tag{28}$$

Therefore, $r = 1$ for two-dimensional flow. This condition is not generally valid in three-dimensional flow. Examples include the Beltrami flows considered in the next section.

4.2 Beltrami Flow
Beltrami flows are flows in which the vorticity vector and the velocity vector are parallel to each other. The outer product of the velocity and the vorticity is zero, i.e., $\epsilon_{ijk} u_j \overline{\Omega}_k = 0$. Applying it to Eq. (24), $\overline{\Omega}_k \overline{\Omega}_{k,i} = \overline{\Omega}_k \overline{\Omega}_{i,k}$. Therefore, $r = 0$ for a Beltrami flow. In this case, Eq. (26) represents Bernoulli's principle for irrotational flow, and Beltrami flow is like irrotational flow.

5. Pressure Field for Unsteady Flow

When the velocity field, u_i is unsteady flow, the velocity field can be expressed as Eq. (10). A typical example is progressive water waves (Shin, 2022, 2023). Using the moving coordinate system proposed by Dean (1965), an unsteady flow can be converted into a steady flow, as presented in the previous Chapter. The moving coordinate system is defined as

$$X_i \overset{\text{def}}{=} x_i - G_i(t) \tag{29}$$

$G_i(t)$ has a length unit. In a damped harmonic oscillator, angular frequency is modified with a damping ratio, "ζ," as shown in Eq. (9). Therefore, the function $G_i(t)$ shows that viscosity also affects the angular frequency of water waves. The first term in Eq. (15) must be a quadratic term of $F(t)$, it is assumed that the function $G_i(t)$ is defined as

$$\dot{G}_j(t) \overset{\text{def}}{=} C_j F(t) \tag{30}$$

where C_j is the phase speed for water waves or a reference speed for other flow, which is a constant. The relative velocity with respect to the moving coordinate system is presented as

$$U_i = u_i - C_i \tag{31}$$

$C_{i,j} = 0$ because C_i is a constant. Hence,

$$\frac{\partial X_i}{\partial x_j} = \delta_{ij} \tag{32}$$

Using Eqs. (29) and (30),

$$\dot{X}_i = -C_i F(t) \tag{33}$$

Using the coordinate system, the velocity field in Eq. (10) can be expressed as

$$v_i(t, x_1, x_2, x_3) = F(t) u_i(X_1, X_2, X_3) \tag{34}$$

The pressure field can be presented by a quadratic function with respect to $F(t)$ as follows:

$$p(t, x_1, x_2, x_3) = \rho S(x_1, x_2, x_3) + F^2 \rho D(X_1, X_2, X_3) \tag{35}$$

where the velocity field u_i is a solution of the Helmholtz equation. Using Eqs. (29), (31), and (33), the local acceleration in Eq. (15) is presented as

$$\frac{\partial u_i}{\partial t} = \frac{\partial u_i}{\partial X_j} \frac{\partial X_j}{\partial t} = -FC_j \frac{\partial u_i}{\partial X_j} = -FC_j \frac{\partial U_i}{\partial X_j} \tag{36}$$

The convective acceleration in Eq. (15) is presented as

$$u_j \frac{\partial u_j}{\partial x_i} = (U_j + C_j) \frac{\partial U_j}{\partial X_i} \tag{37}$$

Differentiating Eq. (35), the gradient of the pressure is presented as

$$\frac{\partial p}{\partial x_i} = F^2(t) \rho \frac{\partial D}{\partial X_i} + \rho \frac{\partial S}{\partial x_i} \tag{38}$$

Substituting Eqs. (36)–(38) into Eq. (15), the result is expressed as follows:

$$\left\{ \frac{\partial S}{\partial x_i} - f_i \right\} + \left(\frac{\partial D}{\partial X_i} + U_j \frac{\partial U_j}{\partial X_i} - \frac{1}{b} \left(\overline{\Omega}_k \frac{\partial \overline{\Omega}_k}{\partial x_i} - \overline{\Omega}_k \frac{\partial \overline{\Omega}_i}{\partial x_k} \right) \right) F^2 = 0 \tag{39}$$

The zero-order perturbation equation is presented as the same in Eq. (19), and the second-order perturbation equation is presented as

$$\frac{\partial D}{\partial X_i} + U_j \frac{\partial U_j}{\partial X_i} - \frac{1}{b} \left(\overline{\Omega}_k \frac{\partial \overline{\Omega}_k}{\partial x_i} - \overline{\Omega}_k \frac{\partial \overline{\Omega}_i}{\partial x_k} \right) = 0 \tag{40}$$

Because $dX_i = dx_i$, integrating the above equation with respect to dx_i gives Bernoulli's principle as follows:

$$D + \frac{1}{2} U_j U_j - \frac{r}{2b} \overline{\Omega}_k \overline{\Omega}_k = Q(t) \tag{41}$$

The dynamic pressure field was determined using Eq. (41). Substituting Eq. (14) into Eq. (30) and integrating the result results in

$$G_j(t) = \frac{C_j}{\mu b} e^{\mu bt} + B \tag{42}$$

where B is an integral constant. For inviscid flow, $G_j(t) = C_j t$ as proposed by Dean (1965); hence, there is a condition to determine the constant.

$$\lim_{\mu \to 0} G_j(t) = C_j t \tag{43}$$

The integral constant is determined as

$$B = -\frac{C_j}{\mu b} \tag{44}$$

6. Results and Verification

Some exact solutions to the NS equations exist for specific conditions (Antuono, 2020; Ethier and Steinman, 1994; Taylor and Green, 1937; Wang, 1991). For verification, the Taylor–Green vortex and Antonio's solution were proven to be specific cases of the general solutions presented in this study.

6.1 General Form of the Velocity Field

A function, $f(x) = e^{ax}$, where "a" is a complex number in this section, satisfies that $f''(x) = a^2 f(x)$. Therefore, the general solution to the Helmholtz equation is presented with a linear combination, i.e.,

$u_i = \sum_{q=1}^{N} A_q \, e^{a_q x_1 - G_1(t)} \, e^{c_q x_2 - G_2(t)} \, e^{d_q x_3 - G_3(t)}$, where a_q, c_q, and d_q are complex numbers in this section, and $b = a_q^2 + c_q^2 + d_q^2$ to satisfy $u_{i,jj} = bu_i$. The coefficients A_q are determined to satisfy Eq. (11), boundary conditions, and initial conditions. The vorticity is also presented with the same form. Three samples are presented in the following sections.

6.2 Vorticity transport equation

Differencing Eq. (2) with respect to x_q and taking the inner product of the result and the Levi-Civita symbol, ϵ_{rqi} with respect to the indices i and q, the vorticity transport equation can be derived as follows.

$$\dot{\Omega}_r + v_j \Omega_{r,j} = \Omega_j v_{r,j} + \mu \Omega_{r,jj} \tag{45}$$

The left-hand side is the material derivative of the vorticity vector. The first term on the right-hand side describes the stretching or turning of vorticity caused by the flow velocity gradients. Eq. (45) can be used as a criterion to judge the validity of the solution because the velocity field has already been determined in the previous section. Substituting Eq. (10) into Eq. (45) and using Theorem 2, the result is as follows.

$$F(t) \dot{\overline{\Omega}}_r + F^2 u_j \overline{\Omega}_{r,j} = F^2 \overline{\Omega}_j u_{r,j} \tag{46}$$

The unsteady case is only considered because unsteady flow contains steady flow. When u_j is unsteady, using the moving coordinate system, Eq. (46) can be expressed as

$$U_j \overline{\Omega}_{r,j} = \overline{\Omega}_j U_{r,j} \tag{47}$$

The first term on the right-hand side in Eq. (47) represents vortex stretching and turning, which is zero for two-dimensional flows. Therefore, Eq. (47) is presented for two-dimensional flows as follows since $\overline{\Omega}_1 = \overline{\Omega}_2 = 0$.

$$U_j \overline{\Omega}_{3,j} = 0 \tag{48}$$

A stream function can be defined as $U_1 = \psi_{,2}$ and $U_2 = -\psi_{,1}$. Therefore, $\Omega_3 = \psi_{,ii}$. $\Omega_3 = \psi_{,ii} = b\psi$ because the stream function is also a solution of Helmholtz equation. Substituting it into Eq. (48), gives

$$U_1 \psi_{,1} + U_2 \psi_{,2} = -U_1 U_2 + U_2 U_1 = 0 \tag{49}$$

Therefore, Eq. (47) is satisfied for two-dimensional flows. $\overline{\Omega}_{j,j} = 0$ and $U_{j,j} = 0$. Hence, Eq. (47) is expressed as

$$\left(U_j \overline{\Omega}_r \right)_{,j} = \left(\overline{\Omega}_j U_r \right)_{,j} \tag{50}$$

For Beltrami flow, i.e., $\overline{\Omega}_i = \phi U_i$, where ϕ is a scalar field, Eq. (50) is satisfied. Therefore, Eq. (47) is satisfied for Beltrami flow. As a result, the solution presented in this study satisfies the vorticity equation.

6.3 Taylor–Green Vortex

The Taylor–Green vortex solution is used to test and validate the temporal accuracy of NS algorithms (Chorin, 1968; Kim and Moin, 1985). Taylor–Green vortex solution (Taylor and Green, 1973) is presented as follows. In the domain $0 \le x_1, x_2 \le 2\pi$, the velocity field is expressed as

$$v_1 = \sin x_1 \cos x_2 F(t) \tag{51}$$

$$v_2 = -\cos x_1 \sin x_2 F(t) \tag{52}$$

where $F(t) = e^{-2\mu t}$. The pressure field is expressed as

$$p = \frac{\rho}{4} \left(\cos 2x_1 + \cos 2x_2 \right) F^2(t) \tag{53}$$

and the vorticity is expressed as

$$\Omega_3 = 2 \sin x_1 \sin x_2 F(t) \tag{54}$$

Eqs. (51)–(54) were cited from Taylor and Green (1937). Therefore, $v_{1,jj} = -2v_1$ and $v_{2,jj} = -2v_2$. The velocity is a solution of the homogeneous Helmholtz equation. Therefore, this study for $b = -2$ gives the Tayor–Green vortex. $\Omega_{3,jj} = -2\Omega_3$, which is a solution of the Helmholtz equation. Because the flow is 2-D, $\overline{\Omega}_1 = 0$, $\overline{\Omega}_2 = 0$, and

$\overline{\Omega}_3 = \overline{\Omega}_3(x_1, x_2)$. Therefore, $\overline{\Omega}_k \overline{\Omega}_{i,k} = 0$, and $r = 1$. Substituting the velocity and vorticity into Eq. (26), the dynamic pressure for $b = -2$ is calculated as follows:

$$D = \frac{1}{4} \left(\cos 2x_1 + \cos 2x_2 \right) + Q - \frac{1}{4}$$

For $Q = 1/4$, the above gives Eq. (53). Therefore, the Taylor–Green vortex is a special case for steady flow in Sec. 4.1.

6.4 Viscous Three-Dimensional Periodic Solution

Antuono's (2020) solutions for three-dimensional problems are defined on a three-dimensional torus $0 \le x_1, x_2, x_3 \le L$ and are characterized by positive and negative helicity, respectively. The solution with positive helicity is expressed as

$$v_i = U_o \left[\sin\left(kx_i - \frac{\pi}{3} \right) \cos\left(kx_j + \frac{\pi}{3} \right) \sin\left(kx_l + \frac{\pi}{2} \right) \right.$$
$$\left. - \cos\left(kx_l - \frac{\pi}{3} \right) \sin\left(kx_i + \frac{\pi}{3} \right) \sin\left(kx_j + \frac{\pi}{2} \right) \right] e^{-3\mu k^2 t}$$

If $i = 1$, then $j = 2$, and $l = 3$; if $i = 2$, then $j = 3$, and $l = 1$; if $i = 3$, then $j = 1$, and $l = 2$. The solution is a sample for steady flow in Sec. 4.2. The velocity field is presented with a linear combination of three trigonometric functions with respect to three variables, x_1, x_2 and x_3. The velocity field is a solution of the Helmholtz equation for $b = -3k^2$ because the linear combination is a solution of the Helmholtz equation. The vorticity field is parallel to the velocity because both solutions belong to the class of the Beltrami flow presented in Sec. 4.2. For the case with positive helicity, the solution is $\Omega_i = \phi u_i$ where $\phi = -\sqrt{3}k$, and the dynamic pressure is given by Eq. (26) for $r = 0$. Antuono's (2020) solutions are also special cases of the solutions presented in Sec. 4.2.

6.5 Two-Dimensional Progressive Water Waves

Using the conventional coordinate system considered in Shin (2022, 2023), the phase is defined as $\beta = kx - \omega t$ where k is the wave number. Therefore, kG corresponds to $\omega t = kCt$ for 2-D inviscid flow. Using Eqs. (42) and (44),

$$kG(t) = \frac{\omega}{\mu b} \left(e^{\mu b t} - 1 \right) \tag{55}$$

Using power series expansion, $kG = \omega t + O((\mu b t)^2)$, where O stands for Big-O notation. Therefore, for inviscid flow, Eq. (55) gives ωt as defined in Shin (2022, 2023). "μb" has a unit of angular frequency. Thus, a dimensionless quantity called the "damping ratio" is defined as $\xi \overset{\text{def}}{=} -\mu b/\omega$. Using the damping ratio, the phase for viscous flow is represented as

$$\beta = kx - \omega t \left\{ \frac{1 - e^{-\xi \omega t}}{\xi \omega t} \right\} \tag{56}$$

Multiplying $e^{-\xi\omega t}$ by the velocity field in Shin (2022, 2023) gave a solution to the NS equation. Multiplying $e^{-2\xi\omega t}$ to the dynamic pressure in Shin (2022, 2023) gives the pressure field for viscous flow. In the conventional coordinate system, the kinematic free surface boundary condition (KFSBC) is presented as

$$v_2 = \frac{\partial \eta}{\partial t} + v_1 \frac{\partial \eta}{\partial x_1} \tag{57}$$

where v_1 and v_2 are horizontal and vertical velocities, respectively, for viscous flow, and η is the wave profile. The KFSBC stipulates that there must be no flow crossing any fluid interface. The free surface, which is a fluid interface, remains unaffected by the viscosity. Consequently, the kinematic boundary condition should remain unaltered by viscosity. Using Eq. (10), the KFSBC is presented as

$$e^{-\xi\omega t}u_2 = \frac{\partial \eta}{\partial t} + e^{-\xi\omega t}u_2\frac{\partial \eta}{\partial x_1} \tag{58}$$

where u_1 and u_2 are the horizontal and vertical velocities, respectively, for inviscid flow. The dimensionless elevation of the wave profile is defined as $\gamma = k(\eta + h)$ in Shin (2022, 2023), where h is the water depth. Using the phase defined in Eq. (56),

$$\frac{\partial \eta}{\partial t} = \frac{\partial \eta}{\partial \beta}\frac{\partial \beta}{\partial t} = \frac{\partial \beta}{\partial t}\frac{d}{d\beta}\left(\frac{\gamma}{k} - h\right) = -\frac{\omega}{k}e^{-\xi\omega t}\frac{d\gamma}{d\beta} \tag{59}$$

and

$$\frac{\partial \eta}{\partial x_1} = \frac{\partial \eta}{\partial \beta}\frac{\partial \beta}{\partial x_1} = \frac{\partial \beta}{\partial x_1}\frac{d}{d\beta}\left(\frac{\gamma}{k} - h\right) = \frac{d\gamma}{d\beta} \tag{60}$$

Substituting Eqs. (59) and (60) into Eq. (58), results in Shin (2022, 2023) because $e^{-\xi\omega t} \neq 0$. The KFSBC in Shin (2022, 2023) is still valid for viscous flow. Applying the dynamic boundary condition on the free surface to Eq. (35), the wave height for viscous flow is expressed as

$$H = H_o e^{-2\xi\omega t} \tag{61}$$

where H_o is the wave height at $t = 0$. Waves emanating from a remote source are referred to as swells, whereas waves produced in the nearby vicinity are termed seas. Specifically, waves formed due to the wind-induced forced oscillation of water are generally identified as seas. In contrast, those originating from the natural oscillation of water post the cessation of wind are labeled as swells. Eqs. (56) and (61) indicate that the height of swell waves decreases when wind energy no longer influences wave formation, leading to a longer wave period and an increase in wavelength over time. The quantity "b" represents the strength of vorticity, σ defined in Shin (2022). $b = -(k\sigma)^2$ because the length is normalized by the wavelength in Shin (2022, 2023). Using $\xi\omega = -\mu b$, the damping ratio is determined as follows:

$$\xi = \frac{\mu(k\sigma)^2}{\omega} \tag{62}$$

A logarithmic decrease is used to determine the damping ratio. Using Eq. (61), the damping ratio can be expressed as

$$\xi = \frac{1}{4\pi}\ln\left(\frac{H_1}{H_2}\right) \tag{63}$$

where H_1, and H_2 represent the wave height of any two successive peaks. Although the strength of vorticity, σ, is determined using the average water particle velocities on the free surface and the seabed in Shin (2022, 2023), it can also be determined using Eqs. (62) and (63), which indicate that the currents considered in Shin (2022, 2023) are generated by the same source as the waves, but they differ from the Stokes drift. This study has proven that viscosity is the source of circulation and current in fluids.

Dean and Dalrymple (1984) provide the decay modulus for long waves with frictional damping as follows:

$$\alpha = \pi P^{1/4} \tag{64}$$

where P is the Proudman number, $P \overset{\text{def}}{=} \mu^2/gk^2h^5$. Shiau and Rumer (1974) carried out a series of experiments to examine the decay of seiches in a basin. The experiments were conducted in very shallow water ($0.15 < h < 8.5$ cm). The theoretical values of α in Eq. (64) were comparable to the experimental data in Fig. 1.

The velocity fields for viscid flows, v_i, were checked. The velocity fields for inviscid flows, u_i, were compared with experimental data by Le Méhauté et al. (1968) in Shin (2022, 2023). Therefore, according to Eq. (10), the function, $F(t)$ was checked instead of the velocity field, v_i, as follows. Eq. (61) is valid for long waves because Shin (2022, 2023) is valid even for ultra-shallow water waves. $\alpha = 2\xi\omega T = 4\pi\xi$ from Eq. (61) because the decay modulus is defined by the relative reduction in amplitude over one wave period. Using Eq. (62), the decay modulus is expressed as

$$\alpha = 4\pi(kh)^2\sigma^2\sqrt{P} \tag{65}$$

Note that $\omega^2 = gk^2h$ for shallow water waves and $\mu = \sqrt{Pgk^2h^5}$. Using Eq. (11) in Shin (2023), Eq. (65) is expressed as

$$\alpha = 4\pi\left\{\cos^{-1}\left(\frac{1 - \bar{u}_s}{1 - \bar{u}_b}\right)\right\}^2 \sqrt{P} \tag{66}$$

where u_s is the average speed in the horizontal direction over a period on still water and u_b is the average speed in the horizontal direction over a period on the seabed. $\bar{u}_s = u_s/C$ and $\bar{u}_b = u_b/C$, where C is the celerity. Upon comparing Eq. (64) and Eq. (66), two distinct differences emerge between these equations. Eq. (64) is based on long-wave theory. Owing to the relatively small water depth in relation
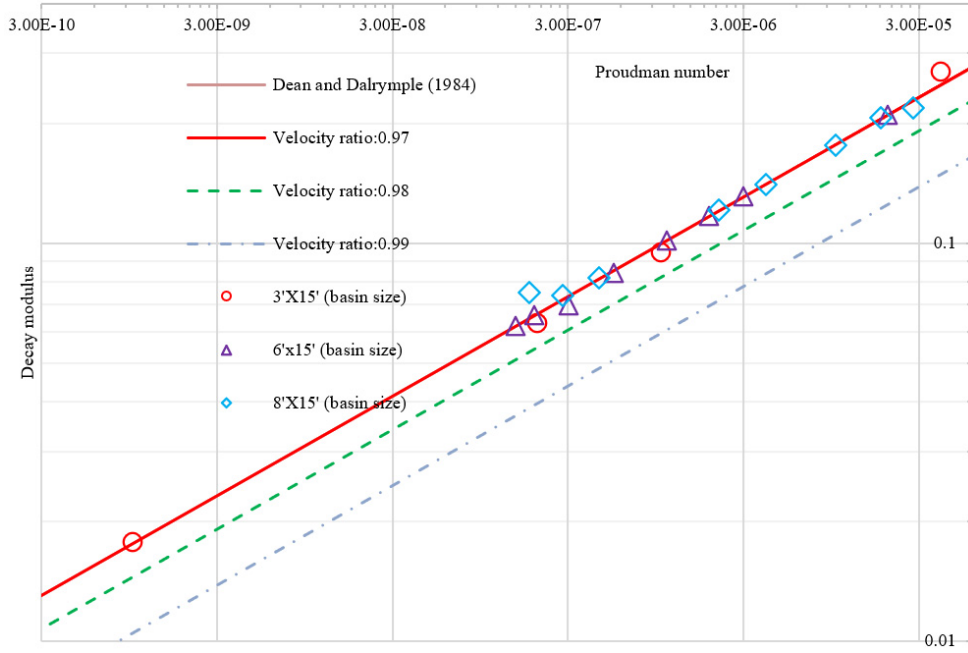
Fig. 1 Decay modulus versus Proudman number [Experiment data from Shiau and Rumer (1974)].

to the wavelength, variations in velocity in the vertical direction were disregarded, and only the average velocity was considered in Eq. (64). Consequently, the decay modulus in Eq. (64) is not dependent on the velocity distribution. On the other hand, the decay modulus in Eq. (66) is closely associated with the velocity distribution. Dean and Dalrymple (1965) used a quadratic friction law where the shear stress is directly proportional to the square of the velocity. The decay modulus in Eq. (64) was calculated assuming that bottom shear stress is presented by $\tau_{12} = \rho\sqrt{\omega\mu}\,u_1$, where u_1 is the horizontal velocity. Therefore, the shear stress is directly proportional to $\sqrt{\mu}$. The present study used a Newtonian fluid model in which shear stress is linearly related to the strain rate, expressed as $\tau_{12} = \rho\mu(u_{1,2} + u_{2,1})$, where x_1 is the horizontal direction and x_2 is the vertical direction. Therefore, the shear stress is directly proportional to μ. Consequently, this leads to a change in the exponent of P from 1/4 to 1/2. When the same constitutive equation and the average concept considered in the long wave theory are used, the average shear stress gradient is as follows.

$$\tau_{12,2} = \rho\sqrt{\omega\mu}\left\{\cos^{-1}\left(\frac{1-\overline{u}_s}{1-\overline{u}_b}\right)\right\}\frac{u_1}{h} \tag{67}$$

Substituting Eq. (67) into the right side of Eq. (13), the decay modulus is presented as

$$\alpha = 4\pi\left\{\cos^{-1}\left(\frac{1-\overline{u}_s}{1-\overline{u}_b}\right)\right\}P^{1/4} \tag{68}$$

For the velocity ratio, $\dfrac{1-\overline{U}_s}{1-\overline{U}_b} = \cos\left(\dfrac{1}{4}\right) = 0.97$, Eqs. (64) and (68) are equivalent to one another, as shown in Fig.1. Eqs. (64) and (68) are

compared in Fig. 1. The comparison results indicated a significant level of concordance between Eq. (64) and Eq. (68). In contrast, this indicates a distinction between Eq. (64) and Eq. (66). The distinction elucidates the rationale behind Dean and Dalrymple's (1965) choice to use a quadratic friction law instead of a Newtonian fluid model. Eqs. (67) and (68) express the applicability of this study even for non-Newtonian fluids, provided that the linearization of shear stresses is achieved using the technique described by Dean and Dalrymple (1984).

7. Conclusions

NS equations play a crucial role in elucidating various scientific and engineering phenomena. They are used in modeling ocean currents, water waves, and other water flows. They help with the design of the structure. Despite the wide range of practical applications, the equations are mainly solved using numerical or experimental methods, while there are some exact solutions to specific problems.

General solutions to NS equations for incompressible flow are presented in this study. The solutions were calculated by combining the solutions of the Helmholtz equation and the solution of a single-degree-of-freedom damped harmonic oscillator. They are analytical exact solutions to NS equations.

The velocity fields and the vorticity fields were presented with solutions of the Helmholtz equations. When the velocity fields are expressed as the product of the solution of the Helmholtz equation and a univariate function of time, the NS momentum equation is decomposed into the Euler momentum equations and an ordinary differential equation for the univariate function of time. The Euler momentum equations were converted to Bernoulli's principle to

determine the pressure field. The time function was determined by solving the ordinary differential equation. Consequently, the general solutions were derived through the linear combinations of the solutions to the Helmholtz equation. The solutions presented in this study are functions of class C^∞ because solutions of the Helmholtz equations are smooth (Lin, 1988).

The Taylor–Green vortex solution and the solutions proposed by Antuono (2020) are particular cases of these solutions, and these solutions satisfy the vorticity equations. The solutions presented by Shin (2022, 2023) were enhanced to integrate viscid water waves with shear currents.

As time elapses or as a swell moves away from its generating area, its height decreases while the period and wavelength increase. Eventually, the swell dissipates entirely because of the removal of the energy source. This phenomenon was substantiated mathematically in the present study. The decay modulus was compared with the experimental data from Shiau and Rumer (1974) and the solution proposed by Dean and Dalrymple (1984). The agreement was excellent. Unlike Dean and Dalrymple (1984), the study showed that the decay modulus is influenced by the velocity gradient in the depth direction.

The technique presented in this study can also be applied to non-Newtonian fluid, provided that the linearization of shear stresses is achieved through the technique described by Dean and Dalrymple (1984).

Conflict of Interest

The author declares that they have no conflicts of interest.

References

BAntuono, M. (2020). Tri-periodic fully three-dimensional analytic solutions for the Navier–Stokes equations. *Journal of Fluid Mechanics*, *890*, A23. https://doi.org/10.1017/jfm.2020.126

Chaplin, J. R. (1980). Developments of stream-function wave theory. *Coastal Engineering, 3*, 179–205. https://doi.org/10.1016/0378-3839(79)90020-6

Chappelear, J. E. (1961). Direct numerical calculation of wave properties. *Journal of Geophysical Research, 66*(2), 501–508. https://doi.org/10.1029/JZ066i002p00501

Chen, H., & Zou, Q. (2019). Effects of following and opposing vertical current shear on nonlinear wave interactions. *Applied Ocean Research, 89*, 23–35. https://doi.org/10.1016/j.apor.2019.04.001

Chorin, A. J. (1968). Numerical solution of the Navier–Stokes equations. *Mathematics of Computation, 22*, 745–762.

Dym, C. L. & Shames, I. H. (1973). *Solid Mechanics: A variational approach.* McGRAW-Hill.

Constantin, A. (2005). A Hamiltonian formulation for free surface water waves with non-vanishing vorticity. *Journal of Nonlinear Mathematical Physics, 12*(1), 202–211. https://doi.org/10.2991/jnmp.2005.12.s1.17

Dalrymple, R. A. (1974). A finite amplitude wave on a linear shear current. *Journal of Geophysical Research 79*(30), 4498–4504. https://doi.org/10.1029/JC079i030p04498

De, S. C. (1955). Contributions to the theory of Stokes waves. *Proceedings of the Cambridge Philosophical Society, 51*(4), 713–736.

Dean, R. G. (1965). Stream function representation of nonlinear ocean waves. *Journal of Geophysical Research, 70*(18), 4561–4572. https://doi.org/10.1029/JZ070i018p04561

Dean, R.G., & Dalrymple, R.A. (1984). *Water wave mechanics for engineers and scientists*. Prentice-Hall, Inc.

Ethier, C. R., Steinman, D. A. (1994). Exact fully 3D Navier–Stokes solutions for benchmarking. *International Journal for Numerical Methods in Fluids, 19* (5): 369–375. https://doi.org/10.1002/fld.1650190502

Henry, D. (2008). On Gerstner's water wave. *Journal of Nonlinear Mathematical Physics, 15*(2), 87–95. https://doi.org/10.2991/jnmp.2008.15.s2.7

Fenton, J. D. (1988). The numerical solution of steady water wave problems. *Computers and Geosciences, 14*(3), 357–368. https://doi.org/10.1016/0098-3004(88)90066-0

Kim, J., & Moin, P. (1985). Application of a fractional-step method to incompressible Navier–Stokes equations. *Journal of computational physics, 59*(2), 308–323. https://doi.org/10.1016/0021-9991(85)90148-2

Kishida, N., & Sobey, R.J. (1988). Stokes theory for waves on a linear shear current. *Journal of engineering mechanics, 114*(8), 1317–1334. https://doi.org/10.1061/(ASCE)0733-9399(1988)114:8(1317

Korteweg, D. J., & de Vries, G. (1895), XLI. On the change of form of long waves advancing in a rectangular canal, and on a new type of long stationary waves. *The London, Edinburgh, and Dublin Philosophical Magazine and Journal of Science, 39*(240), 422–443. https://doi.org/10.1080/1478644950862073

Le Méhauté, B, Divoky, D, & Lin, A (1968). Shallow Water Waves: A Comparison of Theories and Experiments. *Proceedings of 11th Conference of Coastal Engineeing, London, UK* (pp. 86–107). https://doi.org/10.1061/9780872620131.00

Lin, T.-C. (1988). Smoothness results of single and double layer solutions of the Helmholtz equations. *Journal of Integral Equations and Applications, 1*(1), 83–121. https://www.jstor.org/stable/26162915

Nwogu, O. (2009), Interaction of finite-amplitude waves with vertically sheared current fields. *Journal of fluid mechanics. 627*, 179–213. https://doi.org/10.1017/S0022112009005850

Rankine, W. J. M. (1863). VI. On the exact form of waves near the surface of deep water. *Philosophical Transactions of Royal of London 153*, 127–138. https://doi.org/10.1098/rstl.1863.0006

Rienecker, M. M., & Fenton, J. D. (1981). A Fourier approximation method for steady water waves. *Journal of Fluid Mechanics, 104*(1), 119–137.

Shiau, J. C., & Rummer Jr, R. R. (1974). Decay of mass oscillations in rectangular basins. *Journal of the Hydraulics Division, 100(1*), 119–136. https://doi.org/10.1061/JYCEAJ.000384

Shin, J. (2016). Analytical approximation in deep water waves. *Journal*

of Advanced Research in Ocean Engineering, 2(1), 1−11. https://doi.org/10.5574/JAROE.2016.2.1.001

Shin, J. (2019). A regression analysis result for water waves on irrotational flow over a horizontal bed. *International Journal of Offshore and Polar Engineering, 29*(4), 461−466. https://doi.org/10.17736/ijope.2019.hc17

Shin, J. (2022). Solution for water waves with a shear current and vorticity over a flat bed. *International Journal of Offshore and Polar Engineering, 32*(4), 418−423. https://doi.org/10.17736/ijope.2022.hc29

Shin, J. (2023). Numerical method for calculating fourier coefficients and properties of water waves with shear current and vorticity in finite depth. *Journal of Ocean Eng Technol, 37*(6), 256−265. https://doi.org/10.26748/KSOE.2023.034

Stokes, G. G. (1847). On the theory of oscillatory waves. *Transactions of the Cambridge Philosophical Society, 8*, 441−473.

Stokes, G. G. (1880). Stokes, G.G. (2009). *Mathematical and Physical Papers vol.1: Supplement to a paper on the theory of oscillatory waves* (pp. 314−326). Cambridge University Press. https://doi.org/10.1017/CBO9780511702242.016

Skjelbreia, L., & Hendrickson, J. (1960). Fifth order gravity wave theory. *Coastal Engineering Proceedings, 1*(7), 10. https://doi.org/10.9753/icce.v7.10

Taylor, G. I., & Green, A. E. (1937). Mechanism of the production of small eddies from large ones. *Proceedings of the Royal Society A -Mathematical and Physical Sciences, 158*(895), 499−521. https://doi.org/10.1098/rspa.1937.0036

Vanden-Broeck, J. M., & Schwarts, L. W. (1979). Numerical computation of steep gravity waves in shallow water. *Physics of Fluids 22*(10), 1868−1871. https://doi.org/10.1063/1.862492

Wang, C. Y. (1991). Exact solutions of the steady-state Navier−Stokes equations. *Annual Review of Fluid Mechanics, 23*: 159−177. https://doi.org/10.1146/annurev.fl.23.010191.001111

Author ORCID

Author name	ORCID
Shin, JangRyong	0000-0002-0144-2084